American Mineralogist, Volume 68, pages 1102–1112, 1983

Petrochemistry and recrystallization history of granulite xenoliths from the Pali-Aike volcanic field, Chile

JANE SELVERSTONE[1] AND CHARLES R. STERN

Department of Geological Sciences
University of Colorado, Boulder, Colorado 80309

Abstract

Mafic granulite facies xenoliths found in the Pleistocene-Recent alkali basalts of southern Patagonia, South America, have an unfoliated granoblastic matrix with the mineral assemblage clinopyroxene + orthopyroxene + plagioclase ± olivine ± titanomagnetite. Wherever olivine and plagioclase are in close proximity to one another they are separated by symplectic intergrowths of pyroxenes and spinel. Two-pyroxene geothermometry indicates that the granoblastic matrix phases equilibrated at approximately 900°C. The pyroxene–spinel symplectites formed at 860°C, at which temperature the reaction boundary of olivine + plagioclase to produce pyroxenes + spinel occurs at 5–7 kbar. These *P–T* conditions are consistent with *P–T* values previously determined from different generations of fluid inclusions entrapped in both granoblastic matrix and symplectite phases. The xenoliths are interpreted as fragments of a gabbroic pluton which exists at a depth of approximately 20 km in the crust. This is consistent with suggestions that mafic igneous rocks comprise a large portion of the lower continental crust. Capture of the xenoliths in the host basalt must have resulted in extensive heating, but the petrologic evidence of this event is restricted to heterogeneously distributed high temperature oxidation effects.

Introduction

Mafic granulite facies xenolith suites found in alkalic volcanic rocks may potentially provide information concerning the composition and mineralogy of the lower continental crust (for review, see Kay and Kay, 1981). Complex recrystallization histories at depth, followed by transport to the surface in a hot fluid medium, create in such xenoliths petrologic features that need to be unraveled before unambiguous information can be obtained concerning the lower crustal context from which these xenoliths were derived.

This paper describes the petrology of a suite of mafic granulite xenoliths found in the alkali basalts of the Pali-Aike volcanic field of southernmost South America (Skewes, 1978; Skewes and Stern, 1979). The Pali-Aike volcanic field represent the southernmost outcrops of the Patagonian plateau lavas. These lavas are alkali basalts, nephelinites, and hawaiites of Plio-Pleistocene to Recent age which occur as lava plateaus, maars and spatter cones covering large portions of Patagonia east of the High Andean Cordillera.

Basalts in the Pali-Aike volcanic field have brought up abundant xenoliths of both mantle and crustal origin. A wide range of lithologic types is represented by the xenolith suite, including garnet- and spinel-lherzolites, amphibole-bearing peridotites, and dunites, all of presumed mantle origin (Skewes and Stern, 1979). Xenoliths of presumed crustal origin contain dominantly gabbroic granulite assemblages, but less abundant orthopyroxenites, clinopyroxenites, and websterites are also present. The gabbroic granulite xenolith suite from a single cone, Cerro Donoso (Fig. 3 of Skewes, 1978) is the subject of this study. These mafic granulite xenoliths contain textural and mineralogical features which record superimposed events reflecting an extended recrystallization history under changing *P–T* conditions at depth followed by their entrapment and transport to the surface as fragments in the host basalt. The mineral composition data presented here, combined with previously published data for different generations of fluid inclusions preserved in these xenoliths (Selverstone, 1982), allows a detailed reconstruction of the *P–T* history of that part of the lower continental crust from which they were derived.

Information on lower crustal lithologies may also be derived from the *in situ* examination of granulite facies rocks exposed at the earth's surface in regionally metamorphosed terranes. Granulites from regional terranes are, however, typically Precambrian in age and may not be representative of lower crustal lithologies in more recent geologic times. In contrast, no Precambrian base-

[1] Present address: Department of Earth and Planetary Sciences, Massachusetts Institute of Technology, Cambridge, Massachusetts 02139.

0003–004X/83/1112–1102$02.00

ment is known to occur underlying the Pali-Aike volcanic field; the oldest known rocks that have been recovered from drill holes in this region of South America are gneisses which have been dated at 300±150 m.y. (Halpern, 1973). The continental crust through which the Pali-Aike volcanics have erupted has been interpreted as consisting of convergent plate boundary related lithologies accreted to the western margin of Gondwanaland during Phanerozoic times (de Wit, 1977). Moreover, since the host volcanics were erupted less than a million years ago, the granulite nodules from the Pali-Aike volcanic field are representative of deep crustal lithologies currently forming along accretionary plate boundaries.

Petrochemistry and mineralogy

General

The mafic granulite xenoliths (Table 1) from Cerro Donoso contain mineralogical and textural features indicating three superimposed but distinguishable *P–T* stages of evolution. The earliest recognizable stage in the evolution of the xenoliths is represented by the dominant petrologic characteristic of the xenoliths: an unfoliated granoblastic matrix of the mineral assemblage clinopyroxene + orthopyroxene + plagioclase ± olivine ± titanomagnetite. The granoblastic texture, with well developed 120° triple junctions, is indicative of an extensive period of metamorphic recrystallization at elevated temperatures. The absence of any foliation in the granulites suggests that recrystallization occurred under static conditions rather than in response to directional stress. Grain size is generally between 0.5 and 3 mm, but ranges up to 2 cm.

The granoblastic matrix mineralogy of these samples suggests an igneous protolith. Major element chemistry of three samples (Table 2) indicates that the xenoliths do not have compositions that correspond to common igneous rocks; in particular their Na_2O and TiO_2 contents are low. However, these samples do not have the high Al_2O_3 and low MgO contents characteristic of the meta-sedimentary xenoliths from Kilborne Hole, New Mexico described by Padovanni and Carter (1977). The compositions and mineralogy of the Pali-Aike granulites are consistent with their being cumulate rocks, with the relatively incompatible elements like Na_2O, TiO_2 and K_2O having been originally incorporated in interstitial melt rather than cumulate minerals, although no textural evidence for such an origin is preserved. The samples span a range of FeO/(FeO+MgO), with the sample with the highest value containing titanomagnetite as a matrix phase. As discussed below, the chemical variation observed in these three samples reflects not only modal mineralogical variations, but mineral chemistry variations as well.

The next stage in the recrystallization history of the xenoliths is represented by broad zones of symplectic intergrowths of pyroxenes and spinel (see Plate 1 of Selverstone, 1982) which occur separating matrix olivine and plagioclase grains wherever these two minerals are in close proximity to one another. The mafic granulite xenoliths from Cerro Donoso have been divided into spinel-free and spinel-bearing gabbros (Table 1) on the basis of the presence or absence of these spinel–pyroxene symplectite textures. The clear textural evidence that the symplectites are younger than the granoblastic phases implies that the generalized reaction

olivine + plagioclase =

aluminous pyroxenes + spinel (1)

(Kushiro and Yoder, 1966; Green and Ringwood, 1967; Herzberg, 1978) occurred in the solid state during metamorphic recrystallization of the granulites subsequent to the development of the granoblastic textures.

Table 1. Modal mineralogy and temperatures (°C) of equilibration* of Cerro Donoso gabbroic granulite xenoliths

Rock type:	Gabbro			Spinel Gabbro										
Alteration:				Type I					Type II					
Sample #:	2	8	14	1	3	12	18	19	13	16	4	5	11	15
OPX	23	20	25	16	24	26	24	29	16	26	19	10	15	2
CPX	35	25	33	37	28	19	45	46	25	18	43	40	26	29
PLAG	37	53	42	18	36	34	9	8	24	18	24	38	42	35
OL	–	–	–	22	4	8	12	7	28	31	5	2	1	5
SP	–	–	–	5	7	12	5	9	6	6	3	5	6	3
TiMt	–	–	–	–	–	–	–	–	–	–	3	5	7	3
BSLT	6	2	–	2	2	3	5	–	1	–	5	–	3	4
S	–	–	–	–	–	861°†	–	–	–	–	–	–	859°	–
E	943°†	–	–	–	908°	875°	–	–	–	–	–	–	900°	909°
C	917°	–	–	–	–	895°†	–	–	–	–	–	–	896°†	–

OPX = orthopyroxene; CPX = clinopyroxene; PLAG = plagioclase; OL = olivine; SP = spinel; TiMt = titanomagnetite; BSLT = basaltic material in veins as described in text. Percentages based on 500 points per thin section. S = adjacent symplectite pyroxenes; E = edges of adjacent granoblastic matrix pyroxenes; C = cores of adjacent granoblastic matrix pyroxenes.

*Calculated from the two-pyroxene geothermometer of Wood and Banno (1974).

†Averages of temperatures determined from two pairs of pyroxenes.

Table 2. Major element chemistry† of three granulite xenoliths

Sample #	1	2	4
SiO_2	48.99	50.88	46.07
TiO_2	.29	.14	.30
Al_2O_3	14.39	17.32	19.63
FeO*	7.13	5.84	7.16
MgO	12.08	10.87	8.82
CaO	15.71	12.44	15.44
Na_2O	.55	.89	.82
K_2O	.15	.21	.21
Total	99.29	98.59	98.45
FeO/FeO+MgO	.37	.35	.45

†Determined by microprobe analysis of fused glasses.
*Total Fe as FeO.

Microprobe analyses of both matrix and symplectic mineral grains indicate that, in general, granoblastic portions of each sample exhibit chemical homogeneity both within and between grains. Where symplectites are developed between olivine and plagioclase, however, individual matrix grains are zoned from their cores towards their edges in contact with symplectites, and chemical zonation is observed between matrix and symplectic pyroxenes even where their contacts are optically continuous. This suggests that recrystallization of the granulites to produce the granoblastic textures was accompanied by reequilibration and homogenization of the various mineral species; this reequilibration apparently ceased, however, before the *P–T* conditions of the symplectite-producing reaction were reached. Examination and interpretation of these heterogeneities is an important preliminary step to the calculation of pressures and temperatures of equilibration of the xenoliths.

The third distinct stage of evolution of the granulite xenoliths from Cerro Donoso consists of effects related to the entrainment of the xenoliths by the host basalt, their transport to the surface, and/or their history after ejection in the Cerro Donoso spatter cone. These effects include oxidation, which occurs in varying proportions in all the xenoliths, and infiltration of the basaltic host material. Oxidation effects have caused significant variations in the composition of matrix olivine and titanomagnetites but not in other granoblastic matrix or symplectite mineral phases. Infiltration pods of basalt less than 1 mm in diameter are found at triple junction grain boundaries in all samples, and thin stringers of basalt occur lining curvilinear grain margins in a few instances. The infiltration pods typically are composed of subequal amounts of microlitic olivine and plagioclase with subordinate clinopyroxene, set in a matrix of vesicular brown glass which generally occupies 50 percent by volume of each pod. Evidence for partial melting within the gabbroic xenoliths is entirely lacking.

Pyroxenes

Clinopyroxene and orthopyroxene occur as large polygonal matrix grains in both spinel-free and spinel-bearing gabbros, and as symplectic intergrowths with spinel in spinel-gabbros. Matrix orthopyroxene tends to be smaller and more rounded than matrix clinopyroxene. Matrix clinopyroxene grains almost invariably show one direction of fine-scale exsolution lamellae, probably of orthopyroxene, developed near grain margins. Exsolution is less prevalent in orthopyroxene than in clinopyroxene, but patchy exsolution, probably of clinopyroxene, does occur, again primarily near grain margins. Exsolution lamellae are absent from the cores of most matrix pyroxene grains and are totally absent in both pyroxenes where they occur in symplectic intergrowth with spinel. Overall chemical similarities between the two generations of pyroxenes imply that unmixing of the granoblastic pyroxenes occurred prior to the breakdown of coexisting olivine and plagioclase.

Compositions of clinopyroxenes and orthopyroxenes are listed in Tables 3a and 3b respectively. The data are for both the cores and edges of adjacent matrix grains and for symplectic pyroxenes as indicated in the tables.

Pyroxene endmembers were assigned according to the method outlined by Cawthorn and Collerson (1974) for analyses with unknown Fe^{3+}. This technique calculates acmite, and thus Fe^{3+}, in cases where (Na+K) > Al; this situation never occurred in the Pali-Aike samples and all iron is assumed to exist in the ferrous state for all lithologies. Due to high Al_2O_3 and low CaO contents of the orthopyroxenes, Cawthorn and Collerson's (1974) method was modified such that if Ca is insufficient to balance Al in Ca-Tschermak's molecule, Mg-Tschermak's molecule is calculated in an amount necessary to use the remainder of the Al. This was never the case for clinopyroxene analyses, but was applied to all orthopyroxenes.

Ortho- and clinopyroxene data for both granoblastic and symplectic grains, normalized to Wo–En–Fs compositions, are plotted in the pyroxene quadrilateral (Fig. 1) and indicate a general subdivision of the pyroxene suite into two categories on the basis of Fe/(Fe+Mg) ratios. Orthopyroxene of composition En_{76-78} coexists with clinopyroxene with an average composition of $Wo_{48}En_{45}Fs_7$ in both spinel-free and spinel-bearing samples without titanomagnetite. Samples with titanomagnetite exhibit slightly higher Fe/(Fe+Mg) ratios in coexisting pyroxenes, with typical compositions of En_{70-73} and $Wo_{47}En_{40}Fs_{13}$. The titanomagnetite bearing sample for which major element chemistry was determined (#4, Table 2) has higher FeO/(FeO+MgO) than the titanomagnetite-free samples, consistent with the observed change in pyroxene chemistry.

All of the analyzed pyroxenes in the Pali-Aike samples show considerable substitution of non-quadrilateral components, in particular of Al_2O_3, such that use of the standard quadrilateral is not completely adequate for elucidating chemical trends. The high Al_2O_3 and low Na_2O compositions characteristic of pyroxenes in the Cerro Donoso xenoliths are similar to pyroxene analyses of granulite xenoliths from other localities (Wilkinson,

Table 3a. Representative clinopyroxene analyses

	2-1C	2-1E	2-2E	3-3E	11-1C	11-1E	11-2E	11-2S	12-1C	12-1E	12-1S	12-3S	12-4C	15-2E
SiO_2	49.9	51.2	50.2	50.5	49.5	50.2	50.1	50.9	48.3	51.4	51.2	50.0	51.0	49.2
TiO_2	.64	.61	.60	.5	.64	.51	.41	.40	.8	.3	.2	.6	.48	1.25
Al_2O_3	4.9	4.8	4.7	5.5	6.2	6.0	6.4	5.2	6.7	4.5	4.1	6.1	6.5	6.3
FeO^*	5.2	5.4	5.4	4.5	7.3	7.4	8.1	7.0	6.2	5.8	4.7	5.2	5.8	7.9
MgO	14.8	14.7	15.2	14.3	12.5	13.2	13.7	13.3	13.5	14.6	15.8	13.5	13.6	13.1
CaO	23.0	22.2	21.9	22.6	22.7	21.9	20.6	21.9	23.3	23.6	24.6	22.6	22.8	21.6
MnO	.27	.24	.25	.2	.21	.16	.29	--	.2	.3	.2	.2	—	.21
Cr_2O_3	.20	.21	.22	.1	—	—	—	—	.1	—	—	.1	—	—
Na_2O	.85	.88	.88	.6	1.24	1.25	.93	1.45	.7	.7	.7	.9	1.03	.52
Total	99.8	100.2	99.5	98.8	100.2	100.7	100.5	100.2	99.8	101.2	101.5	99.2	101.2	100.1
						atoms per six oxygens								
Si	1.852	1.881	1.865	1.875	1.841	1.853	1.849	1.882	1.801	1.879	1.867	1.857	1.856	1.830
Al^{iv}	.148	.119	.135	.125	.159	.143	.151	.118	.199	.121	.133	.143	.144	.170
Al^{vi}	.066	.089	.070	.115	.113	.128	.127	.110	.096	.073	.044	.124	.137	.106
Ti	.017	.017	.017	.014	.018	.014	.011	.011	.022	.008	.005	.017	.013	.035
Fe^{2+}	.161	.166	.168	.140	.226	.229	.252	.217	.193	.177	.144	.162	.177	.245
Mg	.819	.805	.842	.791	.693	.728	.752	.732	.750	.801	.855	.747	.738	.725
Mn	.009	.006	.006	.006	.007	.005	.009	---	.006	.006	.006	.006	---	.007
Cr	.006	.006	.006	.003	---	---	---	---	.003	---	---	.003	---	---
Ca	.914	.872	.872	.899	.904	.867	.816	.870	.931	.925	.963	.899	.889	.861
Na	.058	.065	.065	.043	.090	.090	.066	.104	.051	.050	.043	.065	.072	.037
mg #	83	83	83	85	75	76	75	77	80	82	86	82	81	75
						pyroxene endmembers								
Wo	40.5	39.0	39.0	40.2	39.3	37.1	34.9	39.0	38.5	41.1	42.4	39.1	38.7	37.7
En	38.9	40.1	40.1	39.0	32.8	34.8	36.3	34.8	35.8	38.6	40.4	36.6	35.7	35.2
Fs	7.6	8.0	8.0	6.9	10.7	10.9	12.1	10.3	9.2	8.5	6.8	8.9	8.5	11.9
Jd	5.5	6.2	6.2	4.2	8.5	8.6	6.4	9.9	4.9	4.8	4.1	6.4	7.0	3.6
CaTs	5.8	5.0	5.0	8.3	6.9	7.3	9.2	4.9	9.5	6.2	5.9	8.2	8.8	8.2
TiTs	1.6	1.6	1.6	1.4	1.7	1.3	1.1	1.0	2.1	0.8	0.5	1.7	1.3	3.4
MgTs	—	—	—	—	—	—	—	—	—	—	—	—	—	—

C = core; E = matrix edge of granoblastic grain; S = symplectite. FeO^*: all Fe calculated as FeO. Mg#=100Mg/Mg+Fe. Endmembers calculated according to the method of Cawthorn and Collerson (1974), modified to include Mg-Tschermak's molecule.

1975; Francis, 1976; McBirney and Aoki, 1973), and to pyroxenes in metamorphosed gabbroic and anorthositic rocks from Norway (Griffin, 1971).

Where orthopyroxene grains grade into symplectites, edge compositions show an increase in Mg-Tschermak's and decrease in Ca-Tschermak's component of between 1 and 3 mole percent from core to edge. Mg numbers (mg = 100Mg/(Mg+Fe)) generally remain constant across each grain. Overall values of Al_2O_3 are lower in symplectites than in cores or edges of matrix grains, suggesting equilibration at lower T or higher P than granoblastic grains (Lane and Ganguly, 1980; Obata, 1976), as discussed in more detail in the following sections.

Symplectic clinopyroxenes exhibit a significant (2.5–5.0 mole %) decrease in Ca-Tschermak's component relative to granoblastic matrix grains, whereas their jadeite content is either the same or greater by up to 3.5 mole percent. Symplectic clinopyroxenes typically have somewhat higher mg numbers than do polygonal grains, which is reflected by an increase in the percentage of enstatite relative to ferrosilite endmembers. Edges and cores of matrix granoblastic clinopyroxenes are unzoned in grains in which exsolution is a minor feature. Where exsolution lamellae are prevalent, generally near grain margins, the ratio of wollastonite to Ca-Tschermak's end-members increases. As the lamellae are on too fine a scale to be analyzed by the electron microprobe, it was not possible to determine whether these chemical variations reflect a true zonation of the pyroxenes or simply a shift in host composition relative to lamellae in a grain of constant bulk composition. Exsolution lamellae are absent from symplectite pyroxenes, implying that recorded chemical differences between lamellae-free cores of matrix grains and the symplectites are real.

Plagioclase

Plagioclase typically occurs as large granoblastic grains, but is embayed where in association with olivine. Twin lamellae are relatively rare, and are discontinuous where present. Plagioclase shows no sign of alteration.

Plagioclase analyses are remarkably similar both between samples and between individual grains within each sample. Compositions range from An_{79} to An_{88} in titanomagnetite-free samples and from An_{71} to An_{77} in the more iron rich titanomagnetite-bearing samples. In all samples plagioclase grains are homogeneous except where in contact with granoblastic clinopyroxene grains; adjacent to clinopyroxene they exhibit reverse zonation of 2–5 mole percent anorthite content within a few tens of microns of the grain boundary. This slight increase in

Table 3b. Representative orthopyroxene analyses

	2-1C	2-1E	2-2E	3-3E	11-1C	11-1E	11-2C	11-2S	12-1C	12-1E	12-1S	12-3S	12-4C	15-2E
SiO_2	53.7	54.0	52.2	54.3	51.7	54.2	51.4	52.7	52.4	52.8	54.2	54.8	53.6	52.8
TiO_2	.29	.18	.14	.1	.12	.12	.15	—	—	.03	—	—	.16	.20
Al_2O_3	3.5	3.4	3.5	4.7	4.1	4.2	4.3	3.5	4.4	3.4	2.4	4.2	3.5	3.8
FeO*	14.4	14.3	14.1	12.0	16.5	16.5	16.7	17.3	15.0	14.8	14.0	14.5	13.6	17.6
MgO	27.6	27.3	27.9	28.5	24.5	24.6	24.9	25.7	28.5	28.8	22.8	26.9	26.9	25.2
CaO	.86	.89	.70	.7	1.17	1.09	1.08	.61	.15	.31	.59	.4	1.13	.80
MnO	.41	.42	.36	.3	.29	.33	.31	.32	.3	.36	—	.5	.52	.34
Cr_2O_3	.14	.14	.11	.1	—	—	—	—	—	.01	—	—	—	—
Na_2O	.01	—	.03	—	.34	.41	.80	.44	—		.34	—	—	—
Total	101.0	100.8	99.2	100.7	98.8	99.6	99.7	100.6	101.1	100.6	99.3	101.3	99.4	100.7
						atoms per six oxygens								
Si	1.911	1.924	1.893	1.909	1.850	1.893	1.866	1.908	1.868	1.889	1.922	1.933	1.904	1.907
Al^{iv}	.089	.076	.107	.091	.150	.107	.134	.902	.132	.111	.078	.067	.096	.093
Al^{vi}	.057	.067	.042	.103	.021	.070	.051	.057	.053	.032	.023	.108	.051	.070
Ti	.008	.005	.003	.003	.003	.003	.004	—	—	.001	—	—	.004	.005
Fe^{2+}	.428	.426	.428	.353	.495	.500	.509	.524	.447	.444	.415	.428	.404	.533
Mg	1.464	1.450	1.513	1.493	1.309	1.327	1.348	1.387	1.514	1.538	1.466	1.414	1.426	1.356
Mn	.012	.012	.012	.009	.009	.010	.009	.010	.006	.011	—	.015	.016	.010
Cr	.003	.003	.003	.003	—	—	—	—	—	—	—	—	—	—
Ca	.034	.034	.027	.026	.045	.042	.042	.023	.019	.012	.022	.015	.043	.031
Na	—	—	—	—	.024	.029	.056	.031	—	—	.023	—	—	—
mg #	77	77	78	81	72	73	73	73	77	78	78	77	78	72
						pyroxene endmembers								
Wo	—	—	—	—	—	—	—	—	—	—	—	—	—	—
En	71.4	71.4	71.8	72.2	65.1	64.8	64.0	62.7	69.6	71.6	73.1	69.0	71.8	65.4
Fs	21.3	21.4	20.9	17.8	25.0	24.9	24.4	25.0	21.5	21.5	20.7	22.0	20.7	26.5
Jd	—	—	—	—	2.4	2.9	5.4	3.0	—	—	2.3	—	—	—
CaTs	3.4	3.4	2.6	2.6	4.6	4.2	4.0	2.2	1.8	1.2	2.2	1.5	4.4	3.1
TiTs	0.8	0.5	0.3	0.3	0.3	0.3	0.4	—	—	—	—	—	0.4	0.5
MgTs	3.1	3.2	4.3	7.0	2.5	2.9	1.7	7.1	7.0	5.6	1.7	7.4	2.7	4.5

C = core; E = matrix edge of granoblastic grain; S = symplectite. Other notes the same as Table 3a.

anorthite content adjacent to clinopyroxenes may reflect breakdown of Ca-Tschermak's component in clinopyroxene in response to a change in *P–T* conditions, thus releasing Ca and Al to the neighboring plagioclase.

Olivine

Olivine is irregular in shape and always associated with green spinel. Where plagioclase is abundant, olivine is embayed and is clearly a relict phase. Where olivine is the more abundant of the two phases, however, it occurs in clusters of grains approximating a granoblastic-polygonal texture; the clusters are embayed and surrounded by spinel in the vicinity of plagioclase. In all cases olivine has been extensively altered by late-stage oxidation processes to either iddingsite or hematite, as described below.

Due to this extensive alteration, few analyses of olivine grains were carried out. Olivines altered to hematite along their edges generally yielded anomalously high FeO and low SiO_2 values, presumably due to interference from fibrous hematite replacing the olivine. Only two such olivines yielded reasonable values for olivine, with mg numbers of 81 and 68; both analyses were made in the relatively hematite-free cores of grains. It is likely, however, that these values are more magnesian than the original olivine compositions due to breakdown of the fayalite component to produce hematite during oxidation, and hence may not represent compositions in equilibrium with pyroxenes and spinel in these samples.

Iddingsite-free cores of olivine grains in samples altered to iddingsite yielded mg numbers between 81 and 75. Again, these analyses may be somewhat more forsteritic than the original olivine due to diffusion of Fe to form iddingsite, but this is probably of less concern in these samples than in olivines altered to hematite. Spot checks with the probe beam across olivine grains altered to iddingsite indicate no significant zonation across the core regions of grains, but a slight increase in MgO content adjacent to iddingsitized margins and fractures. Analyses of cores may thus represent an approximation to the original compositions in equilibrium with spinel and pyroxenes.

Spinel

Spinel is a deep bottle green in color, and occurs both as vermicular grains in spinel-pyroxene intergrowths and as larger discrete grains in the cores of symplectites. In all cases the spinel appears to be a product of the olivine + plagioclase breakdown reaction; there is no evidence for the existence of spinel prior to the occurrence of this reaction.

Spinel compositions are principally confined to the

pleonaste solid solution series between $MgAl_2O_4$ and $FeAl_2O_4$, with an average composition of $Spinel_{60}$ $Hercynite_{40}$ (Table 4). Minor substitution towards calculated Fe^{3+} occupation of the B site does occur, but it is generally confined to spinels which have undergone partial oxidation to hematite, and probably reflects interference of hematite lamellae with the probe analysis of the spinel. One sample (#11) contained highly altered spinels in which (Fe^{total}+Mg) is insufficient to balance Al. Extreme oxidation of spinel to hematite in this sample may have left behind Al-enriched, non-stoichiometric spinels.

Chemical variations exist between vermicular spinels in symplectites and the somewhat larger discrete grains occurring in symplectite cores in the same sample. The symplectic grains are typically more magnesian than discrete grains in the same sample, as reflected by higher mole fractions of the spinel (*sensu stricto*) endmember and correspondingly larger mg numbers. This suggests a sliding boundary for the olivine + plagioclase reaction, such that the more Fe-rich olivine compositions were the first to break down, producing symplectites of relatively hercynitic spinel. As the reaction continued, possibly under changing *P–T* conditions, the early-formed spinels recrystallized into discrete grains and younger, more magnesian symplectites were produced from the more forsteritic remaining olivine. The scale of this difference is ~4 mole percent variation in the $MgAl_2O_4$ endmember of the spinel. No zonation was evident from core to edges of discrete spinel grains.

Considerable variation exists between the mg numbers of spinels from different samples. Although some of this difference is probably due to alteration of spinel to hematite, the three samples in which unaltered spinel was analyzed have average spinel mg numbers between 52 and 64. These variations probably indicate original differences in bulk composition or olivine composition of the samples, and hence may reflect reaction products produced at different points in the *P–T* history of the rock suite as a whole.

Table 4. Representative spinel analyses

	3-1D	3-3S	11-2D	11-2S	12-1D	12-3S	13-I
SiO_2	.01	.10	--	.09	.03	.04	.03
TiO_2	.03	—	.04	.05	--	--	.07
Al_2O_3	63.97	64.86	67.18	66.05	58.52	60.25	50.27
FeO*	17.33	15.63	18.13	17.67	24.53	21.34	21.64
MgO	16.76	17.74	14.13	15.40	14.99	16.89	14.52
MnO	.09	.16	.15	.21	.12	.04	.09
Cr_2O_3	1.40	.64	.26	.25	.55	.07	9.83
CaO	.02	.04	--	.03	—	.03	.02
Total	99.6	99.2	99.9	99.8	98.7	98.7	96.5
cations per four oxygens							
Si	—	.003	—	—	—	—	—
Al	1.953	1.969	2.036	2.005	1.875	1.897	1.686
Ti	—	—	—	—	—	—	.002
Fe2+	.375	.336	.390	.381	.558	.477	.515
Mg	.647	.681	.542	.591	.607	.672	.616
Mn	.002	.003	.003	.005	.003	.001	.002
Cr	.029	.013	.005	.005	.012	.001	.221
Ca	—	.001	—	—	—	—	—
mg #	63	67	58	61	52	58	54
spinel endmembers							
Fe_3O_4	0.9	0.7			8.1	6.6	23.0
$FeCr_2O_4$	1.4	0.6			0.6	—	8.8
$MgAl_2O_4$	64.6	68.1	**	**	59.6	66.1	49.6
$FeAl_2O_4$	32.9	30.3			32.4	27.2	18.3
Fe_2MnO_4	0.2	0.3			0.3	—	—

D=discrete grain; S=symplectite grain; I=inclusion in clinopyroxene. Endmembers assigned according to the scheme outlined by Selverstone (1981). ** = no endmembers assigned due to nonstoichiometry of the spinels; see text for discussion.

Titanomagnetite

Titanomagnetite is an accessory phase in five of the eleven spinel gabbros examined and generally occurs as small grains located at the triple junctions between major phases. In one sample, however, it is also found mantled by green spinel; these overgrowths are found only on titanomagnetite grains closely associated with olivine. As the olivine + plagioclase breakdown does not release Ti, it is unlikely that the titanomagnetite is an additional product of this reaction. Instead, it is possible that titanomagnetite located adjacent to olivine acted as a favorable nucleation site for the spinel produced by the olivine-consuming reaction, thus accounting for the spinel overgrowths.

Late-stage oxidation effects

All of the gabbroic granulite xenoliths have been affected to some degree by late-stage oxidation processes. In the spinel-free gabbros this alteration is confined to black oxidation rims surrounding orthopyroxene grains; clinopyroxene and plagioclase appear unaffected. The spinel-gabbro samples, however, show extensive alteration of olivine and spinel grains, and the members of this suite can be subdivided into two categories on the basis of the type of alteration exhibited (Table 1). Group I samples contain unaltered spinel, but olivine grains show alteration along grain margins and fractures to non-pleochroic bright yellow-orange iddingsite. The absence of any secondary green phyllosilicates suggests that this is Type III iddingsite according to the classification of Baker and Haggerty (1967). Yellow internal reflections visible in the altered olivine under reflected light indicate a goethite component in the iddingsite. This alteration clearly postdates reaction of the olivine to produce spinel–pyroxene symplectites, as the iddingsite exactly parallels even highly irregular grain boundaries and nowhere appears to have been consumed by reaction.

Alteration of Group II samples has been considerably more extensive than that of Group I samples. Spinel grains in the Group II gabbros vary from dark green to almost black in color and are altered to hematite along (111) and, less typically (100) planes. Olivine grains are mantled by hematite rims and exhibit extensive alteration to fibrous hematite in their cores. Small anhedral magnetite grains develop in the cores of particularly strongly altered olivine. The abundance of iron oxides developed

in these olivines suggests that the remaining olivine is probably considerably more forsteritic than was the original composition. Titanomagnetite grains in Group II samples uniformly show alteration to the assemblage pseudobrookite + hematite±black spinel, corresponding to the C7 or most advanced stage of titanomagnetite oxidation, according to the classification scheme of Haggerty (1976).

Geothermometry and geobarometry

Granoblastic matrix and symplectite equilibration

Temperatures calculated according to the equations of Wood and Banno (1973) for pyroxene pairs from symplectic intergrowths, for edge compositions of unexsolved granoblastic matrix pyroxene pairs in contact with one another, and from the core compositions of adjacent granoblastic pyroxene pairs are listed in Table 1. The pyroxene compositions used are those listed in Tables 3a and 3b. The Wood–Banno geothermometer yields average temperatures of 860°C for symplectite pyroxenes, 907°C for edge compositions, and 903°C for cores of grains. An analytical uncertainty of ±5 relative percent in the microprobe determination of Fe and Mg contents of the pyroxenes produces an error of ±35°C in the temperatures calculated according to these models.

It is evident from these data that there is no significant temperature difference recorded by edge compositions versus cores of matrix granoblastic pyroxenes. The symplectite pyroxenes do appear to have equilibrated at somewhat lower temperatures than the granoblastic grains, although there is some overlap between the error limits of temperatures determined from symplectite and edge compositions. This is consistent with temperatures estimated graphically from the Al_2O_3 content of enstatite (Lane and Ganguly, 1980), which fall in the range 775–850°C for symplectic orthopyroxenes and 875–950°C for matrix grains. Although the uncertainties stemming from application of Lane and Ganguly's model, calibrated only for the $MgO–Al_2O_3–SiO_2$ system, to multicomponent pyroxenes are undoubtedly large, the general trend of lower temperatures of equilibration of symplectite pyroxenes calculated by both methods is probably real.

The pressure of equilibration of the granoblastic matrix grains of the Cerro Donoso granulites cannot be determined directly from mineral compositional data, but the pressure of equilibration of the symplectites within the granulites is restricted to the divariant field located between the reaction boundaries for the formation of pyroxenes + spinel from olivine + plagioclase and the breakdown of pyroxenes + spinel to produce garnet. The continued coexistence of olivine and plagioclase in the spinel gabbro samples suggests P–T conditions on or near the univariant curve for Reaction (1). The position in P–T space of Reaction (1) for the $CaO–MgO–Al_2O_3–SiO_2$ system has been experimentally located by several workers (Kushiro and Yoder, 1966; Green and Ringwood, 1967; Herzberg, 1978); extrapolation of these curves to 860°C indicates pressures of 6.5–7.0 kbar for the reaction in the pure endmember system.

Pressures of equilibration of the symplectite phases in the Pali-Aike granulites can be estimated by taking into account the effects of additional components, in particular FeO and Na_2O, on the position of this reaction boundary at constant temperature. At 860°C this results in values of P of 1 to 2 kbar below the pressure for the reaction in the pure endmember system (Selverstone, 1981), suggesting final equilibration of the symplectites in the approximate range of 5 to 7 kbar. This is in good agreement with the fluid inclusion data from symplectite phases (Selverstone, 1982), which indicate a pressure range of 5.0–6.5 kbar for the occurrence of Reaction (1) at the temperature of 860°C determined by two pyroxene geothermometry.

Late-stage oxidation effects

The distinct types of alteration exhibited by Group I and Group II samples suggests that different xenoliths have undergone different late stage oxidation processes. Type III iddingsitized olivines found in Group I samples generally occur in the weathering rinds of basalt and are thought to have originated by weathering processes rather than deuteric alteration. The presence of a goethite component in the iddingsite indicates that the temperature at which oxidation occurred in the Group I samples could not have exceeded 140°C, the thermal stability limit of goethite (Baker and Haggerty, 1967).

Experimental data of Haggerty and Baker (1967) indicate that the direct replacement of olivine and spinel by hematite observed in Group II samples is typical of oxidation under atmospheric conditions at temperatures of 600–820°C. The presence of pseudobrookite as an alteration product of titanomagnetite in these same samples is diagnostic of high temperature oxidation, as members of the pseudobrookite–ferropseudobrookite solid solution series are unstable below 700–800°C (Haggerty and Lindsley, 1969). In contrast to the Group I samples, this implies a high-temperature oxidation origin for the alteration observed in the Group II suite.

Discussion

Protolith emplacement and recrystallization history

The overall similarity in mineralogical and textural features of the spinel gabbro suite suggests that these xenoliths bear a genetic relationship to one another. They are interpreted as resulting from the recrystallization at depth of a clinopyroxene + orthopyroxene + plagioclase±olivine±titanomagnetite gabbro (Fig. 2). This is consistent with the suggestion that mafic igneous rocks may be important constituents of some lower crustal sections

(Ewart *et al.*, 1980; Cox, 1980; Kay and Kay, 1981, and references therein). Chemical diversity in the xenoliths which is expressed mineralogically by the presence or absence of titanomagnetite and the associated variations in silicate mineral chemistry suggests that the protolith gabbroic body may have consisted in part of layered cumulates, although no textural evidence of layering is observed in individual xenoliths. Websteritic and pyroxenetic xenoliths found associated with the gabbroic xenoliths contain pyroxenes which are similar to those of the spinel-gabbros (Fig. 1). These samples may represent more mafic layers from the same protolith body as the gabbroic xenoliths. However, the websterites and pyroxenites generally lack well developed granular textures and may not be related to the gabbroic granulite suite.

Pyroxene geothermometry indicates that the granoblastic-polygonal textures were developed and equilibrated at temperatures above about 900°C. This temperature is higher than expected under conditions of a normal crustal geothermal gradient, suggesting that they developed during cooling of the gabbro body after emplacement into the crust (Fig. 2). Continued cooling to ambient crustal temperatures caused the rocks to cross the reaction boundary for the breakdown of olivine + plagioclase to produce pyroxenes + spinel (Fig. 2). This reaction resulted in the superposition of symplectic textures on the earlier granoblastic texture of the granulites, consistent with the interpretations of Frances (1976) and McBirney and Aoki (1973) for the origin of similar spinel-bearing crustal xenoliths. Two-pyroxene geothermometry indicates that symplectic pyroxenes equilibrated at 860±35°C, at which temperature the reaction of olivine + plagioclase to form pyroxenes + spinel occurs at 5–7 kbar (Fig. 2), consistent with the pressure determined from fluid inclusions entrapped in symplectic pyroxenes (Selverstone, 1982).

Although there are no available mineralogical data with which to calculate pressures of original gabbro emplacement, geological evidence from the Magellanes Basin in which the Pali-Aike basalts occur places constraints on this value. According to Bruhn *et al.* (1978), the last major mafic volcanic–plutonic event in the Magellanes area prior to the eruption of the Pali-Aike alkali basalts took place in the Jurassic, suggesting an age at least that old for the gabbroic protolith of the granulites. Natland *et al.* (1974) indicate deposition of greater than 3000 m of sediments in the Magellanes basin since the onset of subsidence in the Late Jurassic, corresponding to a pressure increase at depth of at least 1 kbar. Working backwards from the pressure of symplectite formation thus indicates gabbro emplacement at pressures of 4–6 kbar (Fig. 2), corresponding to a depth of 12–18 km in the crust. At this pressure, conditions of entrapment calculated from the densities of early-formed CO_2 fluid inclusions are 1100–1200°C, just below the gabbro solidus (Selverstone, 1982). Cooling and recrystallization of Jurassic gabbro intrusions in the lower crust may have been in part responsible for post-Jurassic subsidence in the Magellanes basin.

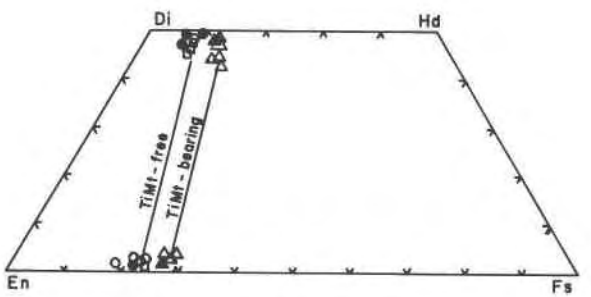

Fig. 1. Diagram showing compositions of coexisting ortho- and clinopyroxenes normalized to Wo–En–Fs components and plotted on the pyroxene quadrilateral. Circles = titanomagnetite-free spinel-gabbros; triangles = titanomagnetite-bearing spinel-gabbros; squares = websterites and gabbros without spinel (Selverstone, 1981). Open symbols = edge and core compositions of granoblastic grains; filled symbols = symplectite compositions.

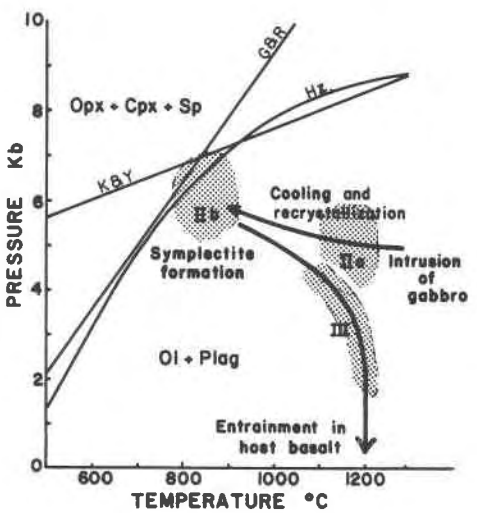

Fig. 2. *P–T* diagram showing path followed by granulites from initial crystallization of a gabbroic protolith, through crystallization during cooling, reaction to produce the symplectites, and final capture and transport to the surface in the host basalt as discussed in the text. Shaded areas indicate calculated *P–T* conditions of entrapment of CO_2 fluid inclusions in granoblastic matrix phases (Type IIa), in symplectite pyroxenes (Type IIb), and late-stage CO_2 + glass inclusions related to penetration of the xenoliths by the host basalt (Type III, Selverstone, 1982). Lines labeled K&Y, G&R, and Hz are uncorrected experimental curves for the reaction olivine + plagioclase to pyroxenes + spinel from Kushiro and Yoder (1966), Green and Ringwood (1967, 1972), and Herzberg (1978).

Interaction of xenoliths with the host basalt

All of the granulite xenoliths examined in this study have been affected to some degree by interaction with the

enclosing basaltic host material which has infiltrated the xenoliths as described previously. However, no evidence has been observed to indicate that any partial melting of the xenoliths occurred. This absence of melt development cannot be interpreted as indicative of lack of heating of the xenoliths by the host basalt. Assuming spherical geometry, a radius of 6 cm for the largest of the xenoliths, and initial temperatures of 850°C for the granulites and 1200°C for the basalts, the time necessary to accomplish complete heating of the xenoliths can be estimated by means of the equation

$$\alpha\theta/r^2 = 0.33 \quad (2)$$

(Schneider, 1963, p. 38), where α is the thermal diffusivity of the rock, θ is the time, and r is the radius of the spherical xenoliths. Using typical values of α between 1.0×10^{-7} and 7.0×10^{-7} m^2/sec (Lienhard, 1981), values of θ determined from Equation (2) range between 0.5 and 3.4 hours. Although this is only an order of magnitude calculation, it indicates that complete heating of the xenoliths in response to the temperature of the enclosing basalt would have occurred in a matter of hours or less (Fig. 2).

Assuming a maximum ascent rate of 1 m/sec for the host alkali basalt (Spera, 1980, estimates 0.5 m/sec based on nodule settling velocities) and a maximum depth of 20 km for the origin of the granulites, travel time in the basalt would have been 5.6 hours. Even at this rapid rate of ascent, complete heating of the xenoliths would have been accomplished in less than half of the time necessary to bring them to the earth's surface. Even had the initial radius of the xenoliths been as much as 30 cm, heating of the cores would have occurred in less than 5 hours. Despite the absence of textural features indicative of partial melting and the metamorphic rather than magmatic temperatures recorded by pyroxene compositions, the xenoliths were certainly subjected to elevated temperatures during their transport history. The absence of melt textures thus probably represents a kinetic rather than a strictly temperature-dependent phenomenon.

McBirney and Aoki (1973), in a study of spinel–gabbro xenoliths similar to those from the Pali-Aike volcanics, noted that the breakdown reaction of olivine and plagioclase to produce two pyroxenes plus spinel had been reversed by reheating of the xenoliths by the host magma. This produced a zone of olivine and plagioclase rimming the pyroxene–spinel symplectites. Evidence for such a reaction reversal is lacking in the Pali-Aike samples with the exception of a few symplectite patches in two samples, in which the spinel is fragmented and surrounded by olivine. Elsewhere in the same samples, however, the symplectites have been unaffected. In fact, the preservation of such fine-scale vermicular intergrowths in rocks that have been subjected to extensive heating is quite remarkable, as it is to be expected that under high temperature conditions recrystallization of the symplectites to more stable grain boundary arrangements would have occurred. Since volume diffusion is time- as well as temperature-dependent, however, the few hours during which the xenoliths were immersed in the hot basalt were obviously not sufficient for extensive recrystallization to have taken place. Also, the volatile content of the granulites may have been too low to have aided in the recrystallization process.

The fact that some of the spinel gabbro xenoliths show only low-temperature oxidation features whereas the basalt appears to have been almost ubiquitously affected by high-temperature oxidation processes suggests that some of the xenoliths may have remained impenetrable to certain volatile species in the basalt. The Group I xenoliths which escaped high-temperature alteration retained assemblages that are particularly unstable at the earth's surface and thus were highly susceptible to the effects of later weathering, resulting in the formation of iddingsite. Since olivine and the opaque minerals in Group II samples were already in a highly oxidized state, weathering processes had little additional effect on them.

The abundance of secondary CO_2 fluid inclusions that appear related to the host basalt (Selverstone, 1982) indicates that at least CO_2 was able to penetrate all of the xenoliths. However, H_2O rather than CO_2 is likely to have been the important volatile species in the oxidation process. Thermodynamic calculations of CO_2 solubilities in typical alkali basaltic magmas indicate that CO_2 is continuously and significantly exsolved from the magma during its ascent and decompression from mantle conditions to the earth's surface (Spera and Bergman, 1980; Eggler, 1975). The data of Eggler, however, indicate that H_2O can remain soluble in the melt until very low pressures (<2 kbar) are reached. Thus, although exsolution of CO_2 from the magma could have caused fracturing of the xenoliths at depth, release of H_2O as a separate volatile species probably occurred nearer the surface and may not have initiated sufficient fracturing to cause high-temperature oxidation of all xenolith cores. The absence of any H_2O-bearing secondary fluid inclusions suggests that H_2O was exsolved from the basalt under such shallow conditions that healing of microcracks, and thus fluid entrapment, was unable to occur.

Summary

Granulite xenoliths brought up by plateau basalts in the Pali-Aike volcanic field indicate the presence of a recrystallized gabbroic body 15–20 km below the surface, consistent with suggestions that lower continental crust consists of a high proportion of mafic bodies. Calculated *P–T* conditions of mineral equilibration of the granulites, combined with data on fluid inclusions and on the post-entrainment heating and ascent rates of the xenoliths, indicate the probable path through *P–T* space followed by these samples from initial crystallization of the gabbroic protolith, through recrystallization processes, up to final

quenching at the earth's surface (Fig. 2). No single approach allows the construction of such a comprehensive picture; it is only by combining the petrologic data with information on fluid entrapment and the ascent of the basalt that such a synthesis is possible.

Acknowledgments

Discussions with James Munoz and Edwin E. Larson, and suggestions by A. P. Jones and R. C. Newton improved various aspects of this study. Alexandra Skewes assisted in the collection of the study material as did the hospitality in Magellanes of Mrs. P. Fell. Ralph Christian of the USGS in Denver provided assistance with the microprobe. Financial support was provided by an NSF graduate fellowship to Selverstone and by NSF grant EAR79 11204. Diagrams were drafted by Karen Schneider.

References

Baker, I. and Haggerty, S. E. (1967) The alteration of olivine in basaltic and associated lavas, Part II: Intermediate and low-temperature alteration. Contributions to Mineralogy and Petrology, 16, 258–273.

Bruhn, R. L., Stern, C. R. and DeWit, M. J. (1978) Field and geochemical data bearing on the development of a Mesozoic volcano-tectonic rift zone and back-arc basin in southernmost South America. Earth and Planetary Science Letters, 41, 32–46.

Cawthorn, R. G. and Collerson, K. D. (1974) The recalculation of pyroxene endmember parameters and the estimation of ferrous and ferric iron contents from electron microprobe analyses. American Mineralogist, 59, 1203–1208.

Cox, K. G. (1980) A model of flood basalt volcanism. Journal of Petrology, 21, 629–650.

de Wit, M. J. (1977) The evolution of the Scotia Arc as a key to the reconstruction of southwestern Gondwanaland. Tectonophysics, 37, 53–81.

Eggler, D. H. (1975) CO_2 as a volatile component of the mantle: the system Mg_2SiO_4–SiO_2–H_2O–CO_2. Physics and Chemistry of the Earth, 11, 401–415.

Ewart, A., Baxter, K. and Ross, J. A. (1980) The Petrology and Petrogenesis of the Tertiary Anorogenic Mafic Lavas of Southern and Central Queensland, Australia—possible implications for crustal thickening. Contributions to Mineralogy and Petrology, 75, 129–152.

Francis, D. M. (1976) Corona-bearing pyroxene granulite xenoliths and the lower crust beneath Nunivak Island, Alaska. Canadian Mineralogist, 14, 291–298.

Green, D. H. and Ringwood, A. E. (1967) An experimental investigation of the gabbro to eclogite transformation and its petrological applications. Geochimica et Cosmochimica Acta, 31, 767–833.

Green, D. H. and Ringwood, A. E. (1972) A comparison of recent experimental data on the gabbro–garnet granulite–eclogite transition. Journal of Geology, 80, 277–288.

Griffin, W. L. (1971) Mineral reactions at a peridotite–gneiss contact, Jotunheimen, Norway. Mineralogical Magazine, 38, 435–445.

Haggerty, S. E. (1976) Oxidation of some opaque mineral oxides in basalts. In D. Rumble, Ed., Mineralogical Society of America Short Course Notes, 3, Hg1–Hg100. Washington, D.C.

Haggerty, S. E. and Baker, I. (1967) The alteration of olivine in basaltic and associated lavas, Part I: high-temperature alteration. Contributions to Mineralogy and Petrology, 16, 233–257.

Haggerty, S. E. and Lindsley, D. H. (1968) Stability of the pseudo-brookite–ferropseudobrookite series. Carnegie Institute of Washington Yearbook, 68/69, 247–249.

Halpern, M. (1973) Regional geology of Chile south of 50° latitude. Geological Society of America Bulletin, 84, 2407–2422.

Herzberg, C. T. (1978) Pyroxene geothermometry and geobarometry: experimental and thermodynamic evaluation of some subsolidus phase relations involving pyroxenes in the system CaO–MgO–Al_2O_3–SiO_2. Geochimica et Cosmochimica Acta, 42, 945–957.

Kay, R. W. and Kay, S. M. (1981) The nature of the lower continental crust: inferences from geophysics, surface geology and crustal xenoliths. Review of Geophysics and Space Physics, 19, 271–297.

Kushiro, I. and Yoder, H. S. (1966) Anorthite–forsterite and anorthite–enstatite reactions and their bearing on the basalt–ecoligite transformation. Journal of Petrology, 7, 337–362.

Lane, D. L. and Ganguly, J. (1980) Al_2O_3 solubility in orthopyroxene in the system MgO–Al_2O_3–SiO_2: a reevaluation and mantle geotherm. Journal of Geophysical Research, 85, 6963–6972.

Lienhard, J. H. (1981) A Heat Transfer Textbook. Prentice-Hall, Inc., New Jersey.

McBirney, A. R. and Aoki, K. (1973) Factors governing the stability of plagioclase at high pressures as shown by spinel–gabbro xenoliths from the Kerguelan Archipelago. American Mineralogist, 58, 271–276.

Natland, M. L., Gonzalez, E., Canon, A. and Ernst, M. (1974) A system of stages for correlation of Magellanes Basin sediments. Geological Society of America Memoir, 139, 1–126.

Obata, M. (1976) The solubility of Al_2O_3 in orthopyroxenes in spinel and plagioclase periodotites and spinel pyroxenite. American Mineralogist, 61, 804–816.

Padovani, E. and Carter, J. (1977) Aspects of the deep crustal evolution beneath South Central New Mexico. In J. Heacock, Ed., The Earth's Crust, p. 19–55. American Geophysical Union Monograph 20. Washington, D.C.

Schneider, P. J. (1963) Temperature Response Charts. John Wiley and Sons, New York.

Selverstone, J. (1981) Petrologic and Fluid Inclusion Study of Granulite Xenoliths, Pali-Aike Volcanic Field, Chile. M.S. Thesis, University of Colorado, Boulder.

Selverstone, J. (1982) Fluid inclusions as petrogenetic indicators in granulite xenoliths, Pali-Aike volcanic field, Chile. Contributions to Mineralogy and Petrology, 79, 28–36.

Skewes, M. A. (1978) Geologia, quimismo y origen de los volcanes del area de Pali-Aike, Magellanes, Chile. Anales del Instituto de la Patagonia, 9, 95–106.

Skewes, M. A. and Stern, C. R. (1979) Petrology and geochemistry of alkali basalts and ultramafic inclusions from the Pali-Aike volcanic field in southern Chile and the origin of the Patagonian plateau lavas. Journal of Volcanology and Geothermal Research, 6, 3–25.

Spera, F. J. (1980) Aspects of magma transport. In R. B. Hargraves, Ed., Physics of Magmatic Processes, p. 265–323. Princeton University Press, New Jersey.

Spera, F. J. and Bergman, S. C. (1980) Carbon dioxide in igneous petrogenesis: I. Aspects of the dissolution of CO_2 in

silicate liquids. Contributions to Mineralogy and Petrology 74, 55–66.

Swanenberg, H. E. C. (1979) Phase equilibria in carbonic systems, and their application to freezing studies of fluid inclusions. Contributions to Mineralogy and Petrology, 68, 303–306.

Wells, P. R. A. (1977) Pyroxene thermometry in simple and complex systems. Contributions to Mineralogy and Petrology, 62, 129–139.

Wilkinson, J. F. G. (1975) An Al-spinel ultramafic-mafic inclusion suite and high pressure megacrysts in an analcimite and their bearing on basaltic magma fractionation at elevated pressures. Contributions to Mineralogy and Petrology, 53, 71–104.

Wood, B. J. and Banno, S. (1973) Garnet–orthopyroxene and ortho-pyroxene–clinopyroxene relationships in simple and complex systems. Contributions to Mineralogy and Petrology, 42, 109–124.

Manuscript received, July 22, 1982;
accepted for publication, April 5, 1983.